

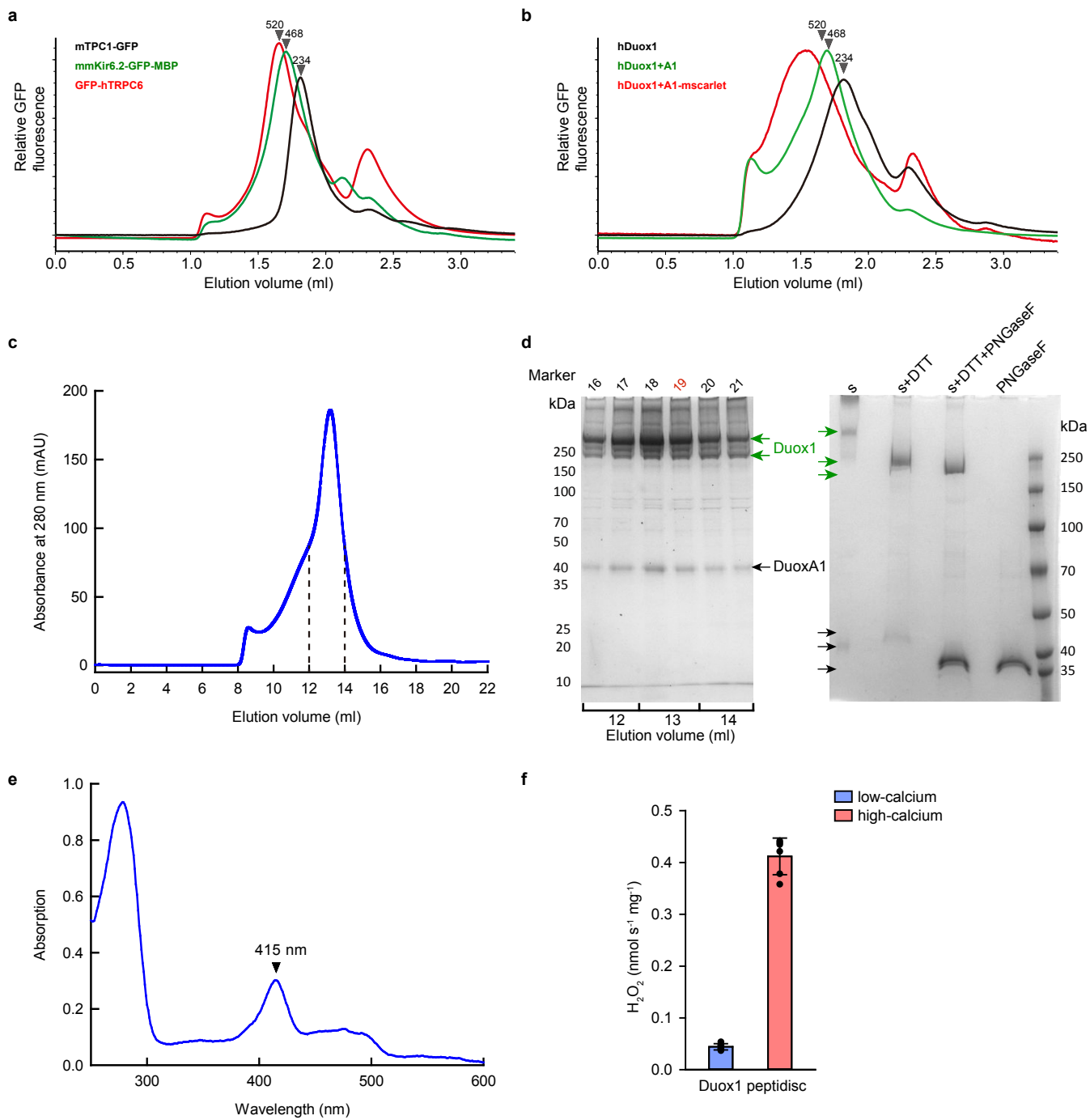
Supplementary Information for

**Structures of human dual oxidase 1 complex
in low-calcium and high-calcium states**

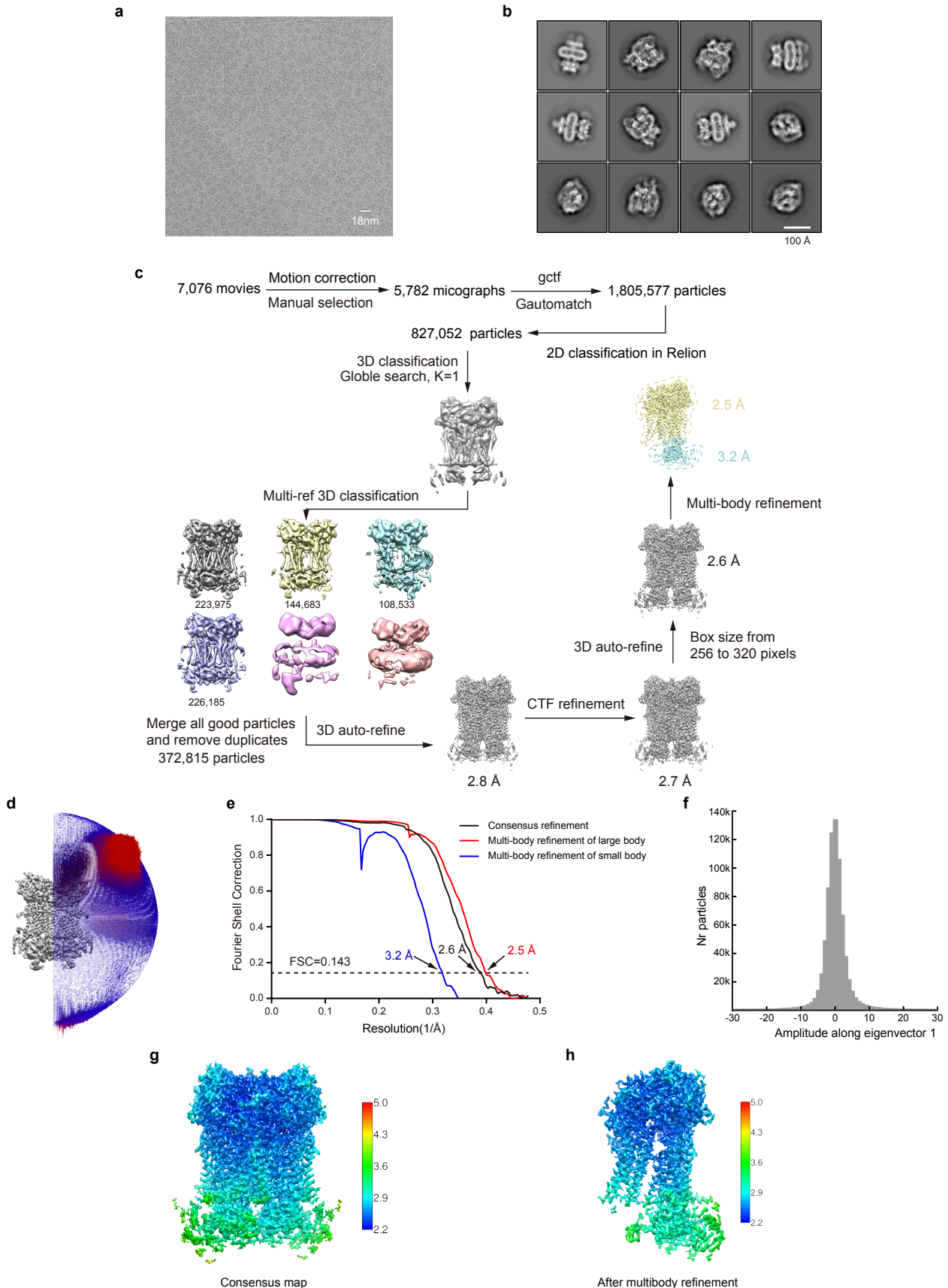
This PDF file contains:

Supplementary Figs. 1-11

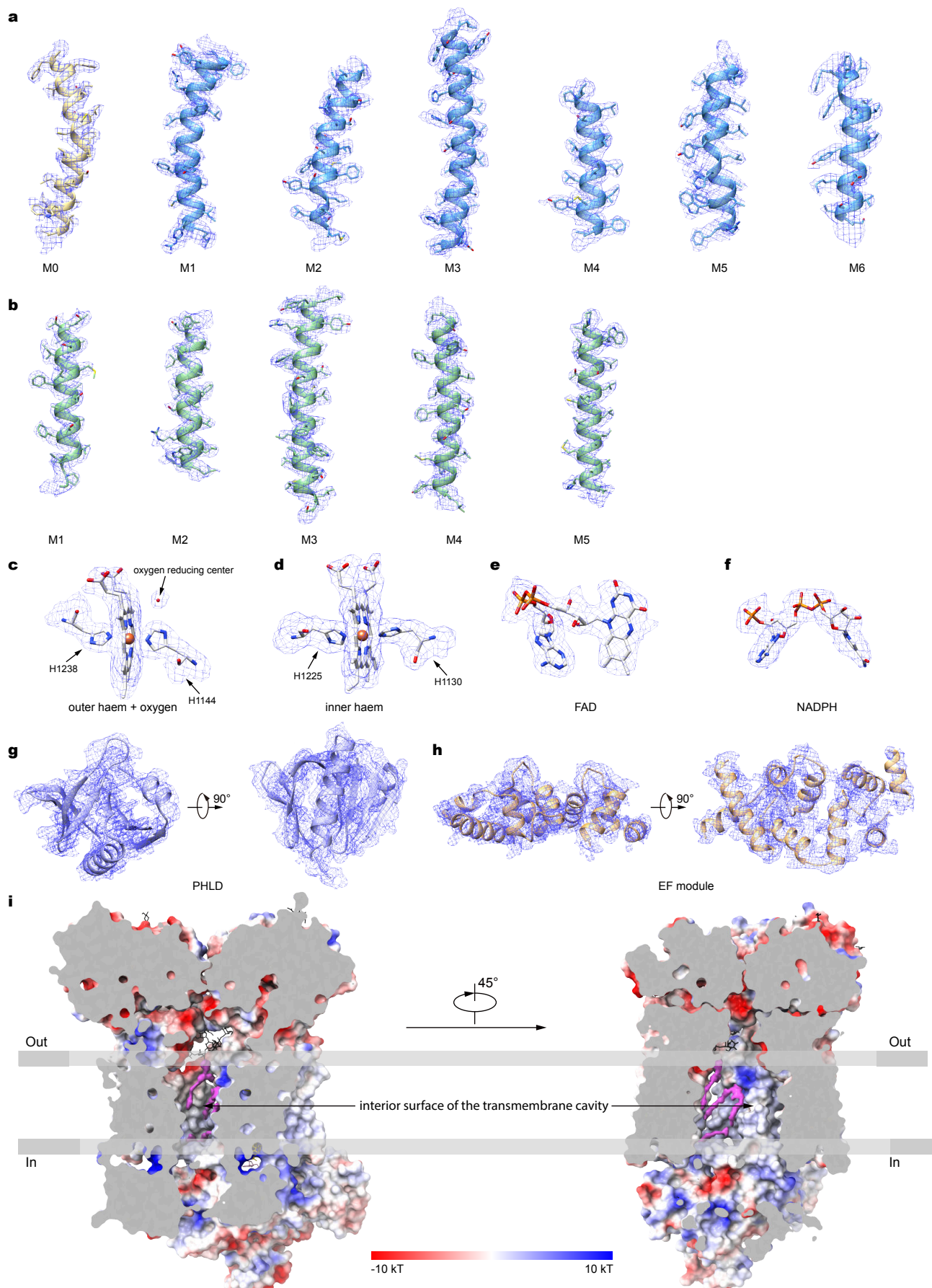
Supplementary Table 1



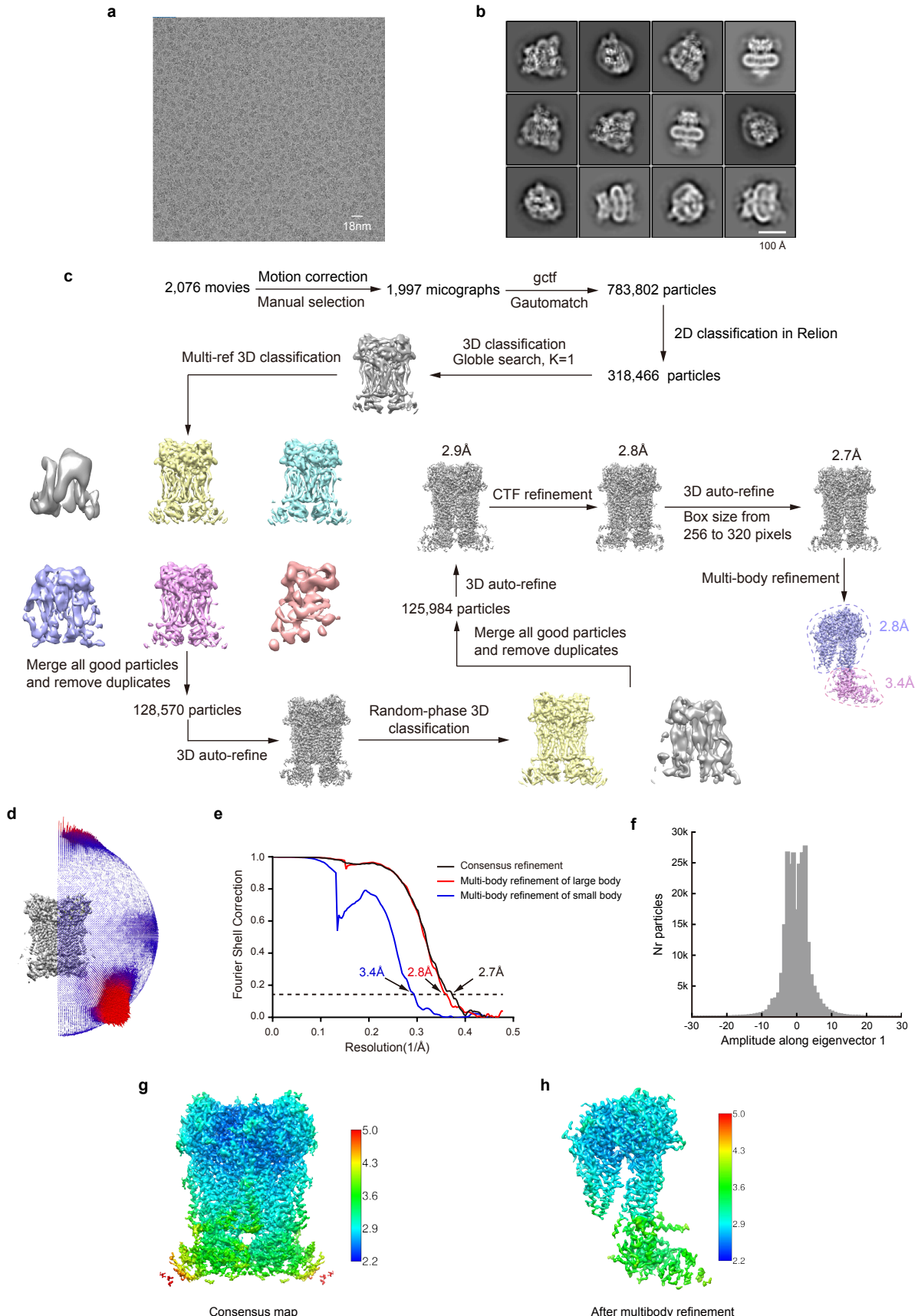
Supplementary Fig. 1 | Biochemical characterization of hDUOX1-hDUOXA1 complex. **a**, FSEC traces of three membrane proteins as molecular weight markers. mTPC1-GFP (234 kDa): mouse TPC1 channel with C-terminal GFP; mmKir6.2-MBP-GFP (468 kDa): Mus musculus Kir6.2 channel with C-terminal MBP-GFP; GFP-hTRPC6 (520 kDa): human TRPC6 with N-terminal GFP. **b**, FSEC traces of hDUOX1 and hDUOX1-hDUOXA1 complex. The positions of the molecular weight markers described in **a** are indicated by arrowheads. hDUOX1: hDUOX1 with N-terminal GFP; hDUOX1+A1: hDUOX1 with N-terminal GFP was coexpressed with nontagged hDUOXA1; hDUOX1+A1-mscarlet: hDUOX1 with N-terminal GFP was coexpressed with hDUOXA1 with C-terminal MBP and msclarlet. **c**, Size-exclusion chromatography of hDUOX1-hDUOXA1 peptidisc complex on a superose 6 column. The fractions indicated by dashed lines were used for SDS-PAGE. **d**, SDS-PAGE of hDUOX1-hDUOXA1 protein samples. SDS-PAGE (left) of the size-exclusion chromatography fractions labeled in **a**. Fraction 19 highlighted in red was concentrated for cryo-EM sample preparation. SDS-PAGE (right) of hDUOX1-hDUOXA1 protein samples treated with DTT or DTT+PNGase F. The positions of hDUOX1 and hDUOXA1 subunits are indicated by green and black arrows, respectively. The original gel was provided as a Source Data file. **e**, UV-Vis spectra of the purified hDUOX1-hDUOXA1 complex. The positions of the Soret peaks are indicated by arrowheads. **f**, Activity of the purified hDUOX1-hDUOXA1 complex peptidisc sample in the presence or absence of calcium. Data are presented as Mean \pm s.d., $n = 6$ biologically independent samples. Source data are provided as a Source Data file.



Supplementary Fig. 2 | Cryo-EM image processing of hDUOX1-hDUOXA1 complex in the high-calcium state. **a**, Representative raw micrograph of hDUOX1-hDUOXA1 in the high-calcium state out of 7,076 micrographs collected. **b**, Representative 2D class averages of hDUOX1-hDUOXA1 in the high-calcium state. Scale bar, 100 Å. **c**, The cryo-EM data processing workflow for hDUOX1-hDUOXA1 in the high-calcium state. **d**, The angular distribution for the consensus refinement of hDUOX1-hDUOXA1 in the high-calcium state. **e**, Gold-standard FSC curves of hDUOX1-hDUOXA1 in the high-calcium state. Resolution estimations are based on the criterion of FSC 0.143 cutoff. **f**, Histogram of the amplitudes along the top eigenvector shows monomodal distribution of hDUOX1-hDUOXA1 in the high-calcium state. **g**, Local resolution distribution of the consensus map of hDUOX1-hDUOXA1 in the high-calcium state. **h**, Local resolution distribution of the composite map of hDUOX1-hDUOXA1 in the high-calcium state after multibody refinement.

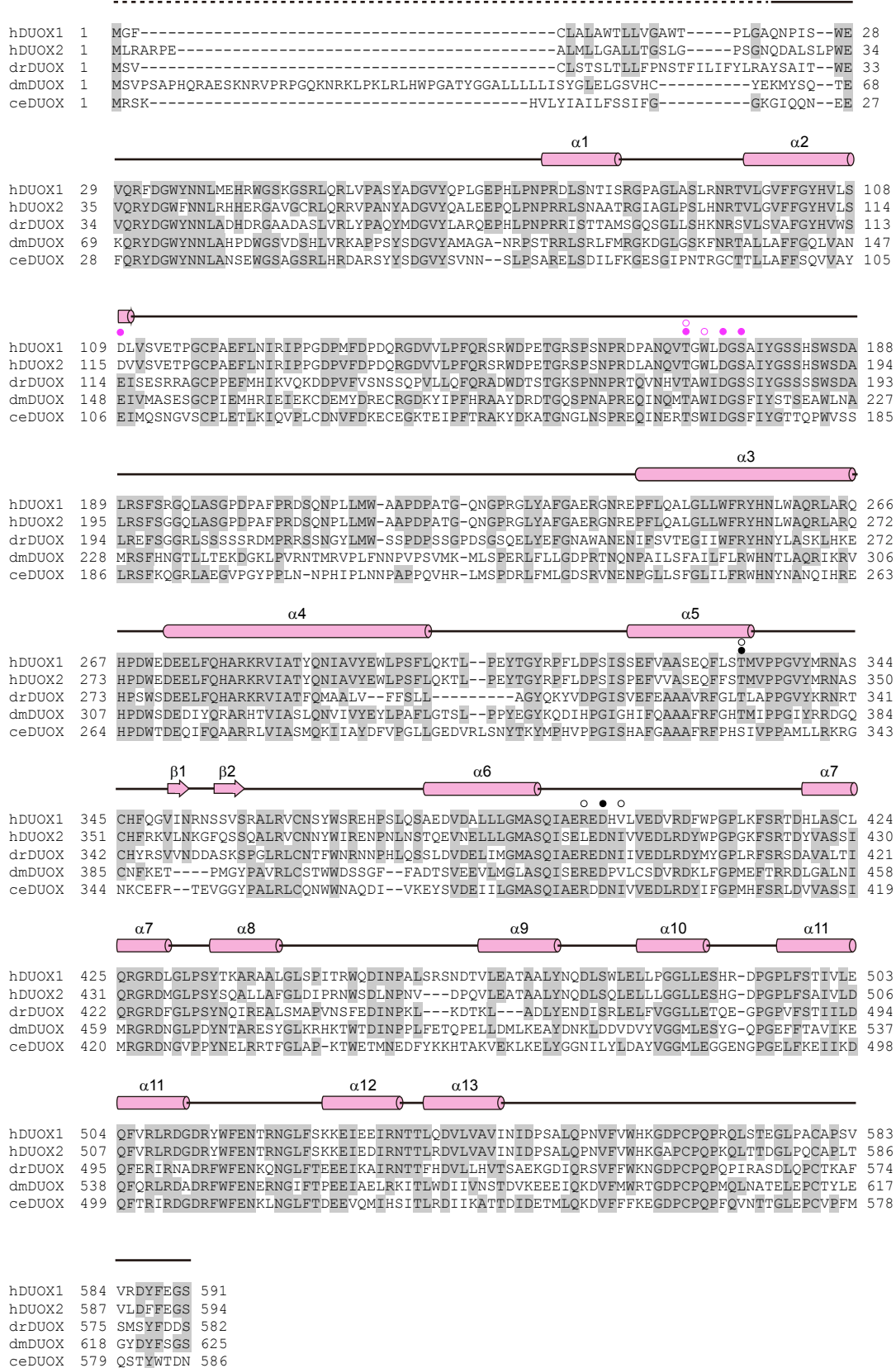


Supplementary Fig. 3 | Representative electron densities of hDUOX1-hDUOXA1 complex in the high-calcium state. **a-b**, Representative densities of transmembrane helices of hDUOX1(**a**) and hDUOXA1(**b**). **c-f**, Representative densities of the outer haem with the interacted histidines and spherical density at the putative oxygen-reducing center (**c**), the inner haem with the interacted histidines (**d**), FAD (**e**) and NADPH (**f**). **g-h**, Representative densities of PHLD (**g**), EF module (**h**). Models of hDuoX1 and hDuoX1A are colored the same as in Fig. 1**h**. The representative densities are all shown in blue mesh. Electron density maps are all contoured at $\sigma=1.86$. **i**, Cross section of the electrostatic surface representation of hDUOX1 shows a large highly hydrophobic central cavity in the transmembrane domain. The surface representation is colored according to electrostatic potential. Putative lipid densities on this surface are shown in magenta.



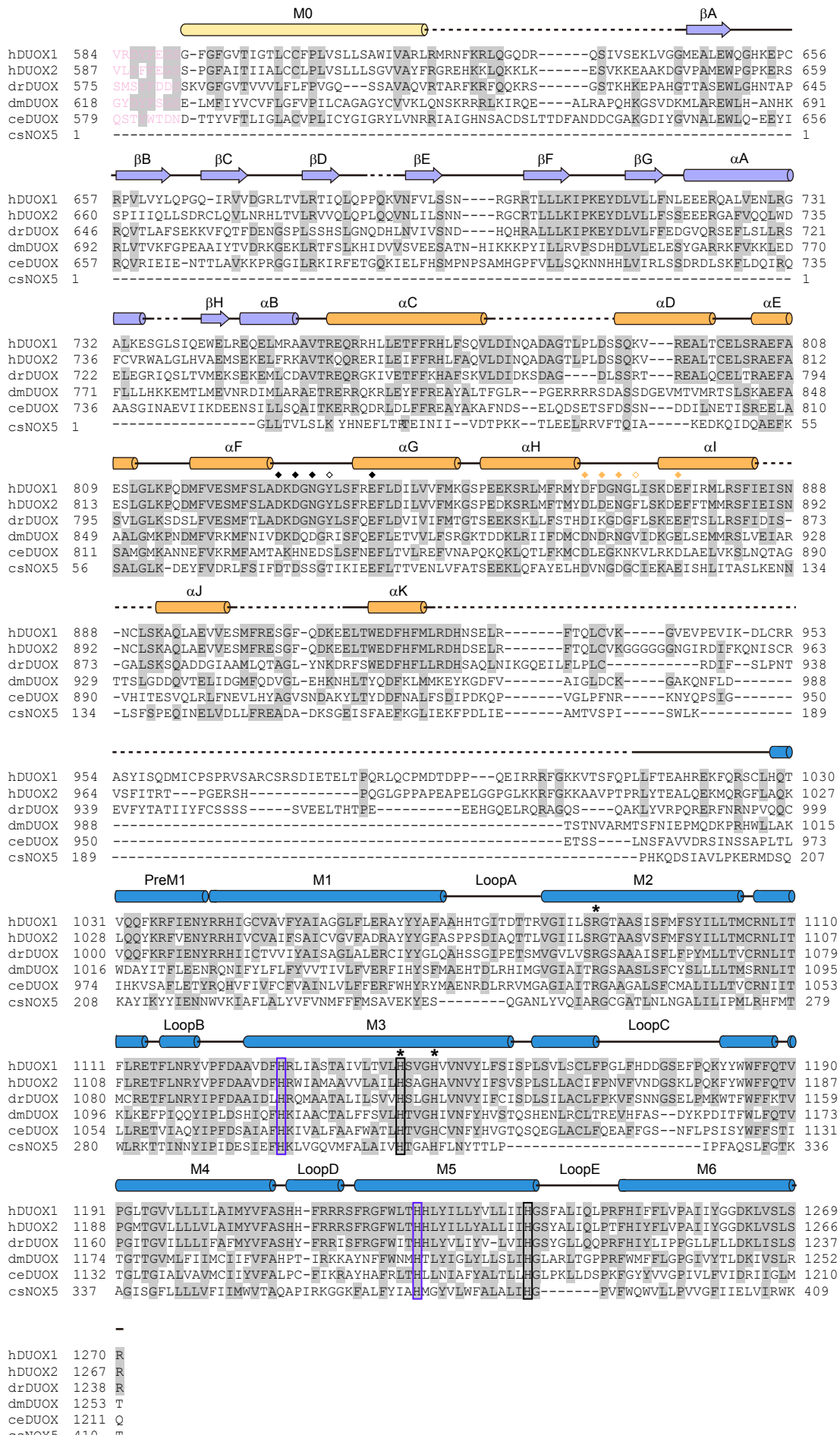
Supplementary Fig. 4 | Cryo-EM image processing of hDUOX1-hDUOXA1 complex in the low-calcium state. **a**, Representative raw micrograph of hDUOX1-hDUOXA1 in the low-calcium state out of 2,076 micrographs collected. **b**, Representative 2D class averages of hDUOX1-hDUOXA1 in the low-calcium state. Scale bar, 100 Å. **c**, The cryo-EM data processing workflow for hDUOX1-hDUOXA1 in the low-calcium state. **d**, The angular distribution for the consensus refinement of hDUOX1-hDUOXA1 in the low-calcium state. **e**, Gold-standard FSC curves of hDUOX1-hDUOXA1 in the low-calcium state. Resolution estimations are based on the criterion of FSC 0.143 cutoff. **f**, Histogram of the amplitudes along the top eigenvector of hDUOX1-hDUOXA1 in the low-calcium state shows a plateau-shaped distribution compared to that of the high-calcium state. **g**, Local resolution distribution of the consensus map of hDUOX1-hDUOXA1 in the low-calcium state. **h**, Local resolution distribution of the composite map of hDUOX1-hDUOXA1 in the low-calcium state after multibody refinement.

DUOX PHD

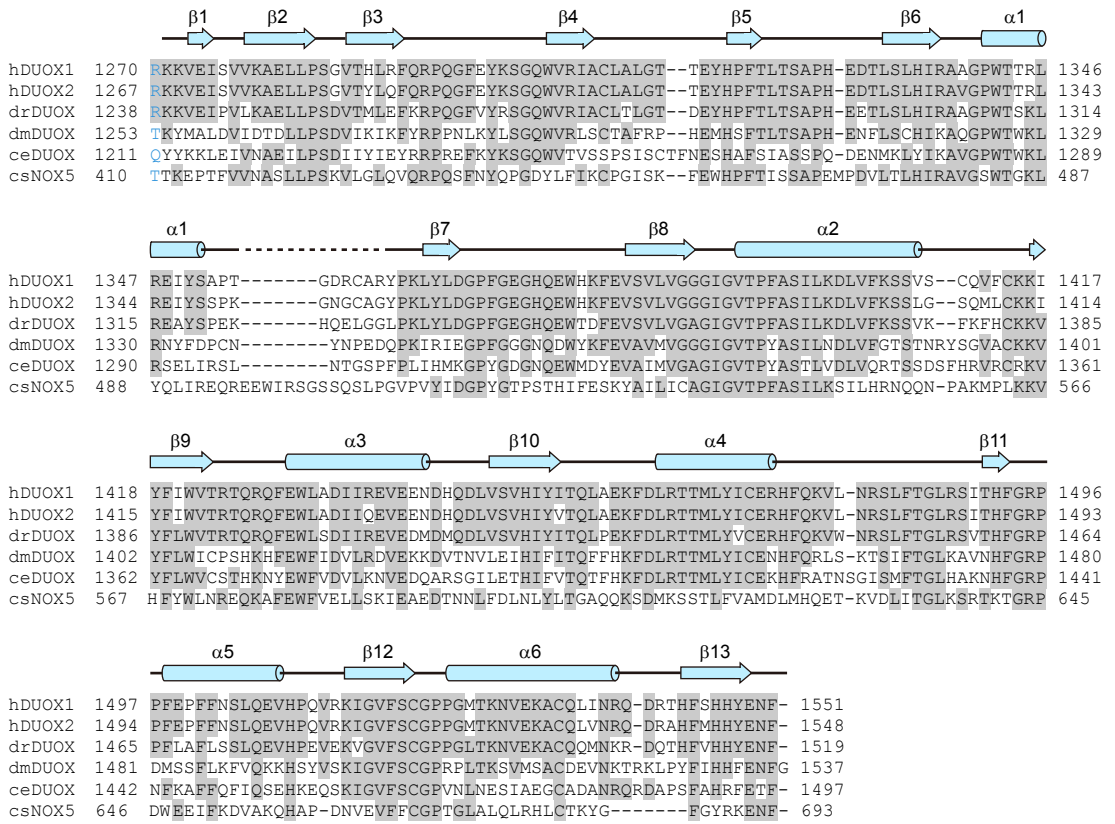


Supplementary Fig. 5 | Sequence alignment of the peroxidase homology domain (PHD) of DUOX. The sequences of the *Homo sapiens* DUOX1 (hDUOX1), *Homo sapiens* DUOX2 (hDUOX2), *Danio rerio* DUOX (drDUOX), *Drosophila melanogaster* DUOX (dmDUOX) and *Caenorhabditis elegans* DUOX (ceDUOX) were aligned. Residues following PHD are omitted for clarity. The sequence alignment of Figs. S5-8 are all shown as follows: Conserved residues are highlighted in gray; Secondary structures are indicated as cylinders (α helices), arrows (β sheets) and lines (loops); Unmodeled residues are indicated as dashed line; The color of arrows and cylinders are the same as in Fig. 1h. Residues of cation binding site 1 (CBS1) and cation binding site 2 (CBS2) are indicated as black circles and violet circles, respectively. The filled circles and empty circles indicate side chain and main chain interactions.

DUOX M0-TMD

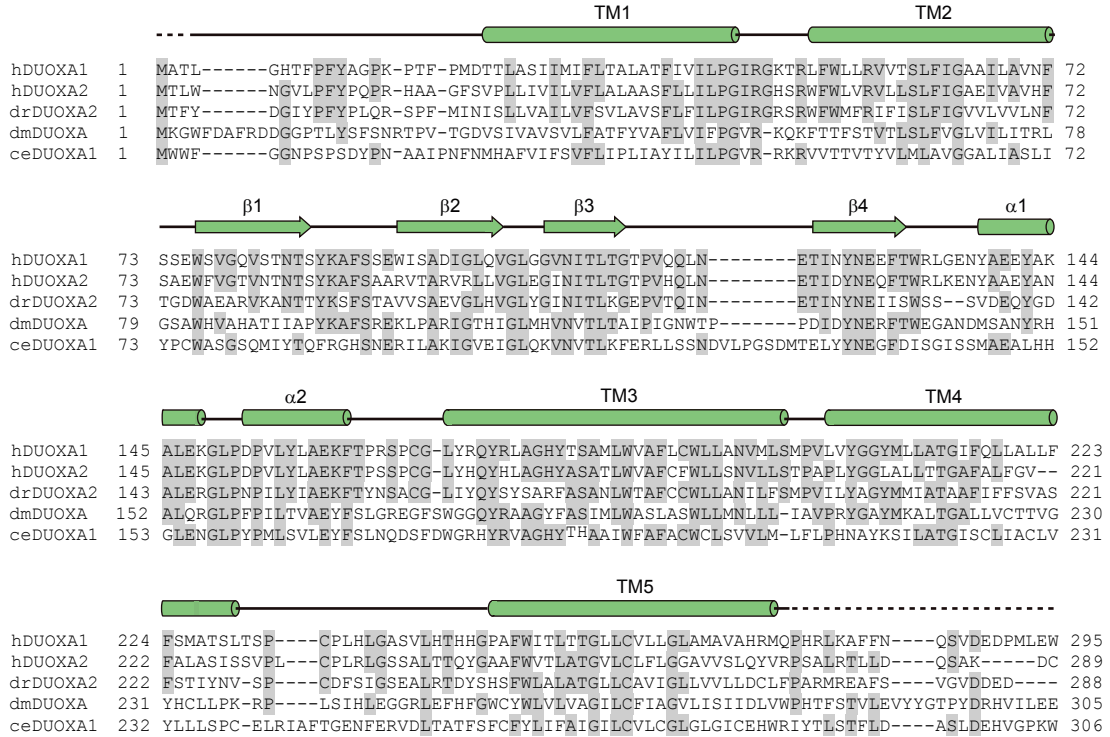


DUOX DH

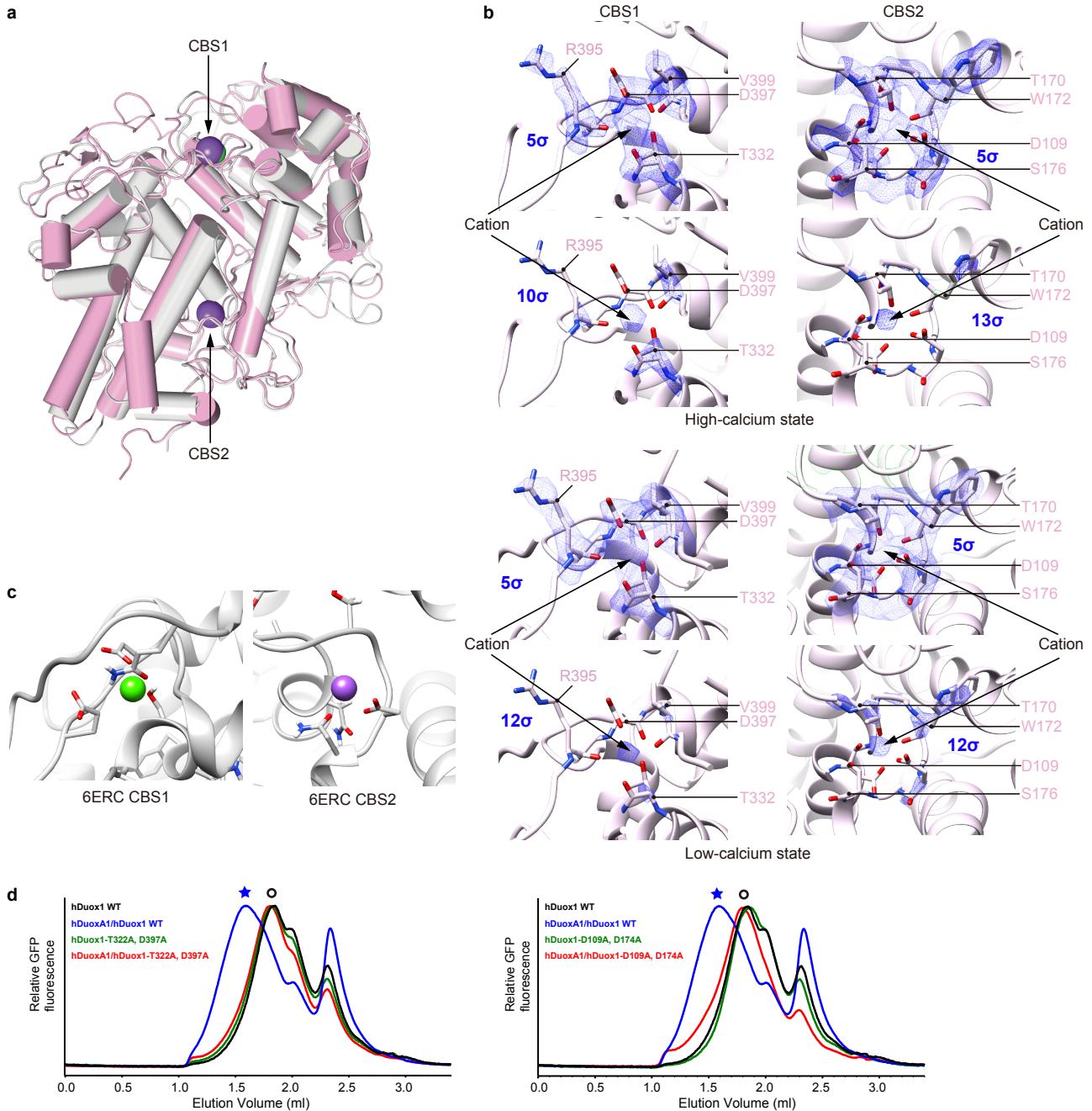


Supplementary Fig. 7 | Sequence alignment of the dehydrogenase domain (DH) of DUOX. The sequences of the *Homo sapiens* DUOX1 (hDUOX1), *Homo sapiens* DUOX2 (hDUOX2), *Danio rerio* DUOX (drDUOX), *Drosophila melanogaster* DUOX (dmDUOX), *Caenorhabditis elegans* DUOX (ceDUOX) and *Cylindrospermum stagnale* NOX5 (csNOX5) were aligned. Residues belonging to TMD are shown in marine. Conserved residues are highlighted in gray. Secondary structures are indicated as cylinders (α helices), arrows (β sheets) and lines (loops). Unmodeled residues are indicated as dashed line. The color of arrows and cylinders are the same as in Fig. 1.

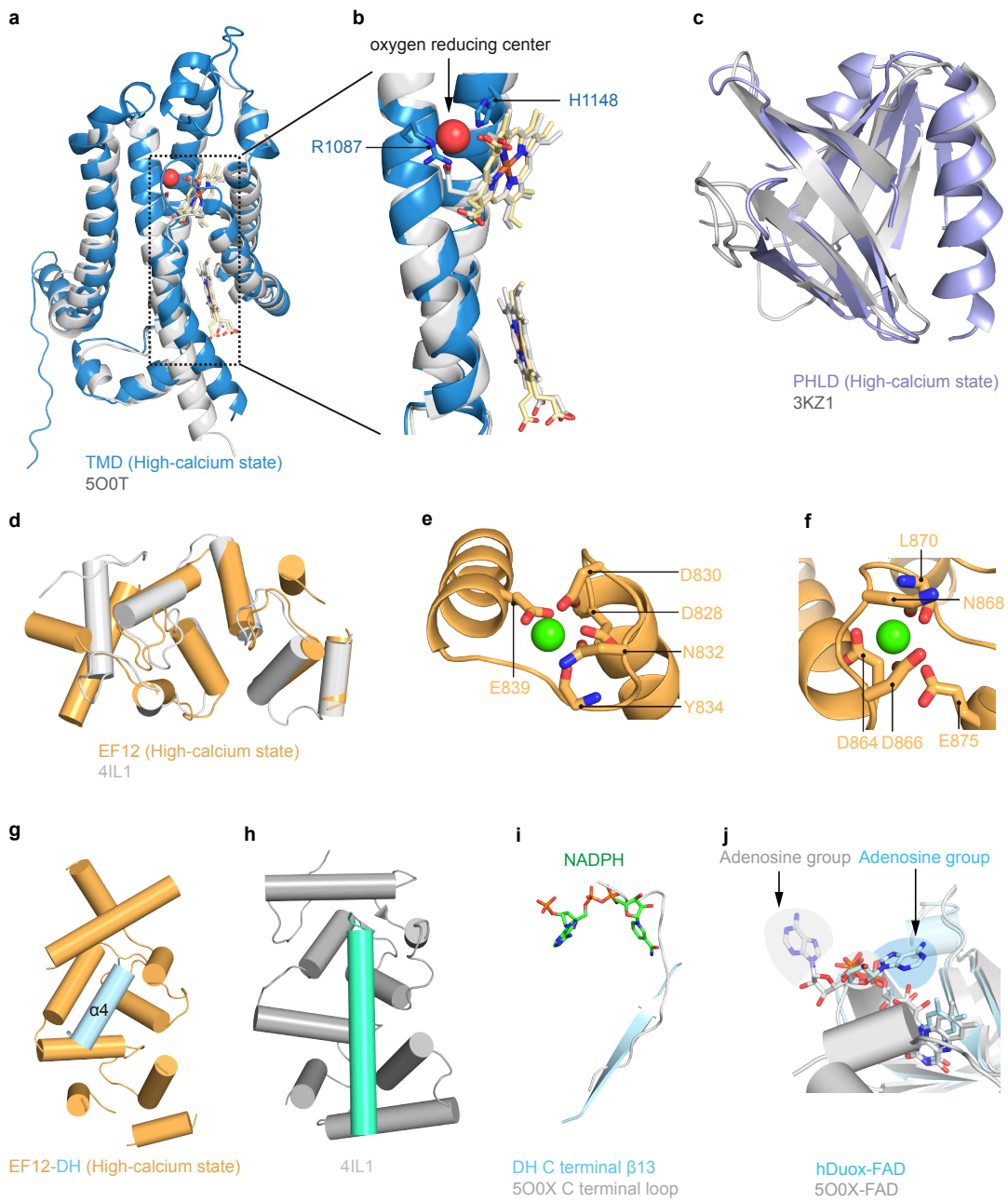
DUOXA



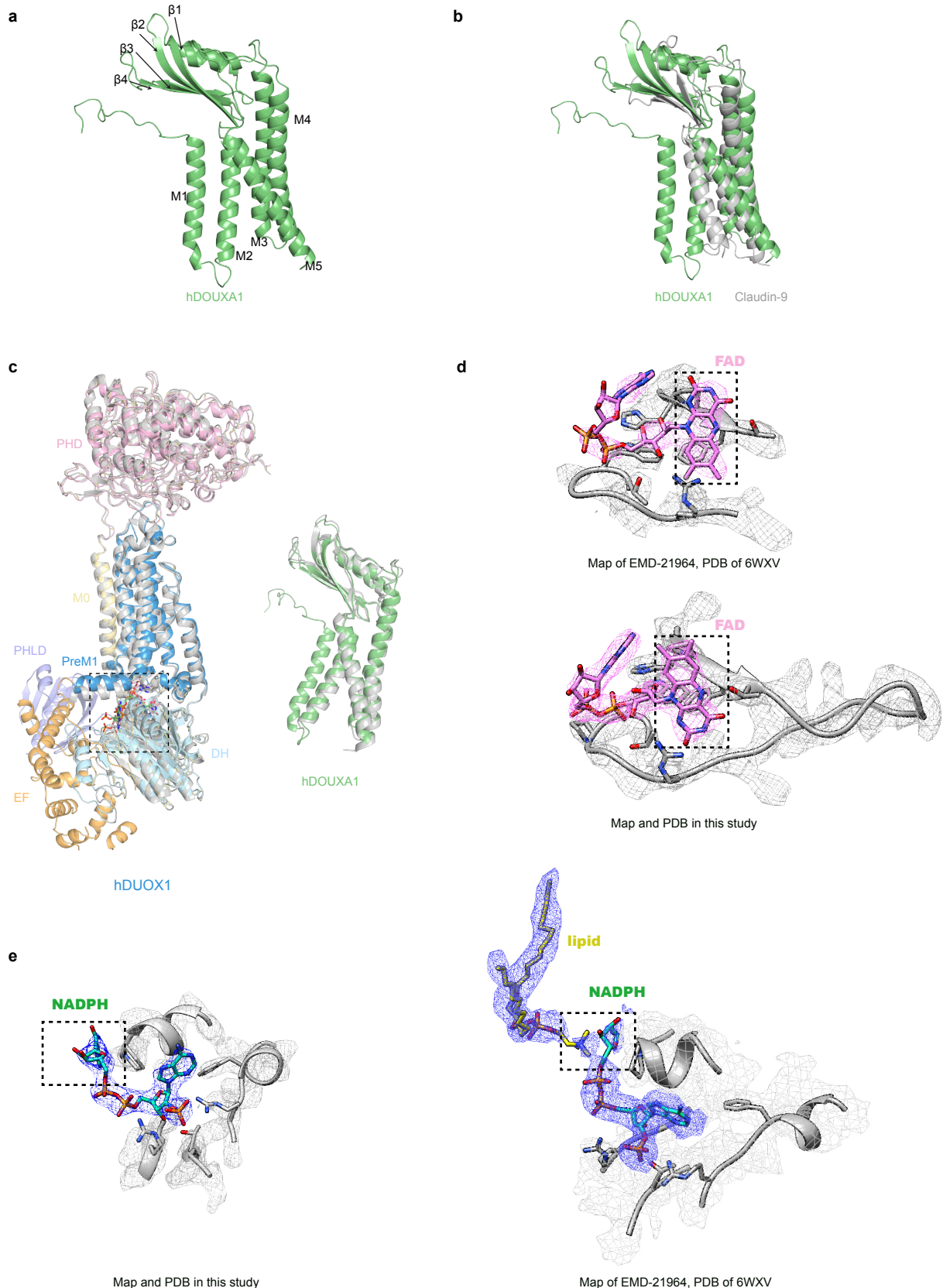
Supplementary Fig. 8 | Sequence alignment of DUOXA. The sequences of the *Homo sapiens* DUOXA1 (hDUOXA1), *Homo sapiens* DUOXA2 (hDUOXA2), *Danio rerio* DUOXA2 (drDUOXA2), *Drosophila melanogaster* DUOXA (dmDUOXA) and *Caenorhabditis elegans* DUOXA1 (ceDUOXA1) were aligned. Conserved residues are highlighted in gray. C-terminal residues are omitted for clarity. Secondary structures are indicated as cylinders (α helices), arrows (β sheets) and lines (loops). Unmodeled residues are indicated as dashed lines. The color of arrows and cylinders are the same as in Fig. 1.



Supplementary Fig. 9 | Structure of hDUOX1 PHD domain. **a**, Structural comparison between hDUOX1 PHD (pink) and DdPoxA (PDB ID: 6ERC, gray). CBS1 and CBS2 are denoted by arrows. **b**, Electron densities (blue meshes) at the cation bound sites under low (top) and high (bottom) contour level in the high-calcium and low-calcium states. The bound cation densities are indicated by arrows. **c**, CBS1 and CBS2 in DdPoxA (PDB ID: 6ERC). **d**, FSEC profiles showed mutations of hDUOX1 CBS1 (T322A, D397A) or CBS2 (D109A, D174A) affect hDUOX1-hDUOXA1 tetramer assembly. Asterisks denote the peak position of tetrameric complex and circles denote hDUOX1 monomer peak position.



Supplementary Fig. 10 | Structure of hDUOX1 TMD and cytosolic domains. **a**, Structural comparison between hDUOX1 TMD (blue) and csNOX (PDB ID: 500T, gray). The putative oxygen-reducing center is shown as red sphere. **b**, The close-up view of the similar architecture of the putative oxygen-reducing center. **c**, Structural comparison between hDUOX1 PHLID (light blue) and PDZ-RhoGEF (PDB ID:3KZ1, gray). **d**, Structural comparison between hDUOX1 EF module (orange) and Calcineurin B subunit (PDB ID: 4IL1, gray). **e**, Calcium binding on EF1 domain. Calcium ion is modeled according to 4IL1 and shown as green sphere. **f**, Calcium binding on EF2 domain. Calcium ion is modeled according to 4IL1 and shown as green sphere. **g**, Structure of hDUOX1 EF module (orange) in complex with α4 helix (light blue) of DH domain. **h**, Structure of calcineurin B subunit in complex with helix of calcineurin A subunit (PDB ID: 4IL1). **i**, Structural comparison of NADPH binding pocket between hDUOX1 (colored) and csNOX (PDB ID: 500X, gray). Only β13 and NADPH are shown for clarity. **j**, Structural comparison of FAD binding pocket between hDUOX1 (colored) and csNOX (PDB ID: 500X, gray). The large rotations of adenosine group of FAD are denoted by arrows.



Supplementary Fig. 11 | Structure of hDUOXA1 subunit. **a**, Structure of hDUOXA1 subunit with secondary structure labeled. **b**, Structural comparison of hDUOXA1 with claudin-9 (PDB ID:6OV2). hDUOXA1 is colored in green and claudin-9 is colored in gray, respectively. **c**, Structural overlay of DUOX1 (left) and DUOXA1 (right) subunits between hDUOX1 in our study (colored) and mDUOX1 published by other group (PDB ID: 6WXV, gray). Dashed lines indicate the substrate binding sites, enlarged in **d-e**. **d-e**, Detailed structural comparison of modeled FAD and NADPH molecules.

Supplementary Table 1 | Cryo-EM data collection, refinement and validation statistics

PDB ID EMDB ID	High-calcium state 7D3F EMD-30556	Low-calcium state 7D3E EMD-30555
Data collection and processing		
Magnification	130,000 ×	130,000 ×
Voltage (kV)	300	300
Electron exposure (e-/Å ²)	50	50
Defocus range (μm)	-1.5 to -2.0	-1.5 to -2.0
Pixel size (Å)	1.045	1.045
Symmetry imposed	C2	C2
Initial particle images (no.)	1,043,262	783,802
Final particle images (no.)	372,815	125,984
Map resolution (Å)	2.6 (2.5/3.2)*	2.7 (2.8/3.4)*
FSC threshold	0.143	0.143
Map resolution range (Å)	250.0-2.5	250.0-2.8
Refinement		
Initial model used (PDB code)	6ERC, 5O0T, 4IL1, 5O0X	
Model resolution (Å)	2.5	2.8
FSC threshold	0.5	0.5
Model resolution range (Å)	250.0-2.5	250.0-2.8
Map sharpening <i>B</i> factor (Å ²)	(-98.1/-153.3)*	(-76.0/-122.2)*
Model composition		
Non-hydrogen atoms	26,466	26,012
Protein residues	3,282	3,304
Ligands	46	42
Water	2	2
<i>B</i> factors (Å ²)		
Protein	69.42	113.39
Ligand	61.83	108.21
Water	60.06	109.22
R.m.s. deviations		
Bond lengths (Å)	0.004	0.004
Bond angles (°)	0.927	0.945
Validation		
MolProbity score	1.68	1.45
Clashscore	6.64	6.87
Poor rotamers (%)	2.58	0.44
Ramachandran plot		
Favored (%)	98.24	97.70
Allowed (%)	1.76	2.30
Disallowed (%)	0.00	0.00

* The numbers outside the brackets are from the consensus refinement. Numbers inside brackets are from the multibody refinement (large body/small body).

Supplementary Table 2 | Primers used in this study

Primer Name	Sequene
hDUOX1_21_NGFP_F	CAAGGCCCTGAATTGggagctcagaacccatt
hDUOX1_FL_C.stop_R	GTGGTGGTGCTCGAGctagaagttcataatggtg
hDUOXA1_FL_N_F	ATATGAATTCatggctactttggga
hDUOXA1_FL_C.stop_R	ATATCTCGAGtataaagcacaatcaggatcttgggtgtgcctcittacagtatgccttggtaggaaag
hDUOXA1_FL_C_R	CAGGTTTCCTCGAGtaaagcacaatcagg
hDuox1_R507A_F	cttgaacaatttgtGCgtacggatgg
hDuox1_R507A_R	accatcccgtagcGCcacaaatttgtcaag
hDuox1_R507E_F	cttgaacaatttgtGAgctacggatgg
hDuox1_R507E_R	accatcccgtagcTCcacaaatttgtcaag
hDuox1_R50E_F	ggcagecaaaggctcGAgctgcagcgcctg
hDuox1_R50E_R	caggcgctgcagcTCggagccttgctgcc
hDuox1_T332AD397A_F	gagcagtccgtccGccatggccccct
hDuox1_T332AD397A_R	aaccaacacatggGcctctcgctctgcat
hDuox1_D109AD174A_F	tatcacgtgcattcagCcctggtagcgtg
hDuox1_D109AD174A_R	gatggcgctgcggGccagccagccgtcac